

1

2 PROF. DONG-IL KIM (Orcid ID : 0000-0002-5313-9554)

3

4

5 Received Date : 25-Mar-2020

6 Revised Date : 29-Jun-2020

7 Accepted Date : 02-Jul-2020

8 Article type : Research Letter

9

10

11 **TC-E 5003, a protein methyltransferase 1 inhibitor, activates the PKA-**
12 **dependent thermogenic pathway in primary murine and human subcutaneous**
13 **adipocytes**

14 **Min-Jung Park^a, Jiling Liao^{b,c,d} and Dong-il Kim^{a,d*}**

15 ^aDepartment of Physiology, College of Veterinary Medicine, Chonnam National University, Gwangju,
16 61186, Republic of Korea; ^bGerontology department, Beijing Hospital, National Center of Gerontology;
17 ^cInstitute of Geriatric Medicine, Chinese Academy of Medical Sciences, Beijing, 100730, China; ^dLife
18 Sciences Institute, University of Michigan, Ann Arbor, Michigan, 48109, USA

19

20

21 *To whom correspondence should be addressed.

22 Dong-il Kim, Email: kimdi@chonnam.ac.kr

23 Department of Veterinary Physiology, Rm206, College of Veterinary Medicine Bd1, Chonnam

This is the author manuscript accepted for publication and has undergone full peer review but has not been through the copyediting, typesetting, pagination and proofreading process, which may lead to differences between this version and the [Version of Record](#). Please cite this article as [doi: 10.1002/1873-3468.13900](https://doi.org/10.1002/1873-3468.13900)

This article is protected by copyright. All rights reserved

24 National University, 77 Yongbong-ro, Buk-gu, Gwangju, 61186, Korea
25 Phone: +82-62-530-2832, Fax: +82-62-530-2809

26

27 **Abstract**

28 We previously reported the involvement of protein arginine methyltransferase 1 (PRMT1) in adipocyte
29 thermogenesis. Here, we investigate the effects of PRMT1 inhibitors on thermogenesis.
30 Unexpectedly, we find that the PRMT1 inhibitor TC-E 5003 (TC-E) induces the thermogenic
31 properties of primary murine and human subcutaneous adipocytes. TC-E treatment upregulates the
32 expression of *Ucp1* and *Fgf21* significantly and activates protein kinase A signaling and lipolysis in
33 primary subcutaneous adipocytes from both mouse and human. We further find that the thermogenic
34 effects of TC-E are independent of PRMT1 and beta-adrenergic receptors. Our data indicate that TC-
35 E exerts strong effects on murine and human subcutaneous adipocytes by activating beige
36 adipocytes via PKA signaling.

37 **Keywords:** thermogenesis; PRMT1; UCP1; PKA; lipolysis

38

39 **Abbreviations**

40 WAT: white adipose tissue

41 UCP1: uncoupling protein1

42 ATP: adenosine triphosphate

43 cAMP: cyclic adenosine monophosphate

44 PKA: protein kinase A

45 PRMT1: protein arginine methyltransferase 1

46 TC-E: TC-E 5003

47 SVF: stromal vascular fraction

48 iWAT: inguinal white adipose tissue

49 ISO: isoproterenol

50 iBAT: interscapular brown adipose tissue

51 eWAT: epididymal white adipose tissue

52 HSL: hormone-sensitive lipase

53 AP1KO: adipocyte-specific PRMT1 knockout mice

This article is protected by copyright. All rights reserved

54 SQ: subcutaneous

55 CARM1: coactivator-associated arginine methyltransferase 1

56

57 **Highlights**

- 58 ◆ TC-E treatment increases the expression of *Ucp1* mRNA in primary iWAT cells.
- 59 ◆ TC-E treatment activates the downstream molecules of PKA signaling.
- 60 ◆ Thermogenic effects of TC-E are PRMT1- and β -adrenergic receptor-independent.
- 61 ◆ TC-E potently works in human SQ adipocytes isolated from multiple donors.

62

63 **1. Introduction**

64 Thermogenic adipocytes found in adult humans [1-3] are heterogeneous. A considerable portion of
65 cells resembles murine beige adipocytes [4,5], although some of the other cells are similar to murine
66 brown adipocytes [6,7] Murine beige adipocytes are distinct from the classic brown adipocytes and
67 reside in subcutaneous (SQ) white adipose tissue (WAT). These adipocytes consume energy in the
68 form of heat by breaking down the proton gradient across the inner mitochondrial membrane by using
69 uncoupling protein 1 (UCP1) without the generation of adenosine triphosphate (ATP) [8]. Hence, the
70 understanding of the mechanism underlying the activation of beige adipocytes is important to
71 overcome obesity and associated metabolic disorders.

72 Beige adipocytes are primarily activated by cold-mediated sympathetic activation, resulting in the
73 release of norepinephrine from the nerve ending innervated in the WAT. One of the well-characterized
74 subtype of cold-activated adrenergic receptors of murine adipocytes is the β 3-adrenergic receptor that
75 activates adenylyl cyclase which catalyzes the conversion of ATP to cyclic adenosine monophosphate
76 (cAMP) [8]. An increase in the level of intracellular cAMP promotes the activation of protein kinase A
77 (PKA), which subsequently increases *Ucp1* transcription. Thus, the signaling cascade, β 3-adrenergic
78 receptor–adenylyl cyclase–cAMP–PKA, is the canonical pathway involved in the activation of
79 thermogenic adipocytes [9].

80 Using genetic approaches, we recently demonstrated the strong involvement of protein arginine
81 methyltransferase 1 (PRMT1) in beige adipocyte thermogenesis [10]. As PRMT1 is also associated
82 with the progression of many types of cancers, diverse drugs that inhibit PRMT1 activity have been
83 discovered [11,12]. However, their effects on beige adipocyte thermogenesis have not been
84 elucidated. In the present study, we tested four different inhibitors of PRMT1 and found that one of
85 them, TC-E 5003 (TC-E), exerted strong effects by activating beige adipocytes via PKA signaling.

86

87 **2. Materials and Methods**

88 **2.1. Reagents**

89 TC-E 5003 (Tocris; 5099), furamide dihydrochloride (Tocris; 5202), AMI-1 (Cayman; 13965),
90 MS023 (Cayman; 18361), isoproterenol (ISO; Sigma; I6504), cAMP (Sigma; D0627), and H-89
91 (Cayman; 10010556) were purchased.

92 **2.2. Primary murine cell cultures**

93 To obtain primary cells, murine inguinal WAT (iWAT) or interscapular brown adipose tissue (iBAT)
94 was isolated, minced with sharp surgical scissors, and digested in a 37°C shaking (200 rpm) water
95 bath using collagenase D/dispase II (Roche; 11088882001, 4942078) or collagenase B/dispase II
96 (Roche; 11088831001) solution, respectively. After filtration with a 100 µM mesh, the separated cells
97 were centrifuged. The pellet obtained was re-suspended and filtered again with 40 µM mesh before
98 another centrifugation step. The pellet containing the stromal vascular fraction (SVF) was re-
99 suspended in DMEM/F12 glutaMax (Life Technologies; ILT10565042) supplemented with 15% FBS
100 and penicillin/streptomycin and seeded on collagen-coated plates. For adipogenic differentiation, the
101 cells seeded on 12-well collagen-coated plates were stimulated with modified differentiation media
102 (DMEM/F12 glutaMax instead of DMEM) for 2 days and then maintained in modified maintenance
103 media (DMEM/F12 glutaMax instead of DMEM). The medium was changed every other day. On day
104 6, the cells were used for experiments. To obtain primary epididymal WAT (eWAT) cells, SVF was
105 obtained from murine eWAT in a manner similar to that for iWAT SVF. The cells were seeded on
106 collagen gel and differentiation was induced as previously described [13].

107 Primary PRMT1 knockout iWAT cells were prepared from adipocyte-specific PRMT1 knockout
108 (AP1KO) mice that were generated by breeding a PRMT1^{fl/fl} mouse, that were kindly provided by
109 Seung-Hoi Koo (Korea University), with an adiponectin(AQ)-Cre recombinase mouse (Jackson
110 Laboratory; 010803). Cells isolated from PRMT1^{fl/fl};AQ^{+/+} were used as wild-type (WT), while those
111 obtained from PRMT1^{fl/fl};AQ^{Cre/+} served as AP1KO. PRMT1^{fl/fl} mice used in this study were
112 backcrossed to 6J background for more than 10 generations. The β-less primary iWAT cells were
113 isolated from β-less mice that were kindly provided by Dr. Bradford Lowell (Harvard Medical School).
114 Animals were maintained in accordance with the protocol reviewed and approved by the University
115 Committee on Care and Use of Animals at the University of Michigan. Detailed methods are provided
116 in Supplementary methods.

117 **2.3. Human cell cultures**

118 Human adipose precursor cells isolated from the SQ fat were obtained as previously described [14].
119 All specimens were collected under the protocols reviewed and approved by the University of
120 Michigan Medical School Institutional Review Board (IRBMED). Undifferentiated cells were cultured in
121 MesenPRO RS medium (Life Technologies; 12746012) supplemented with penicillin/streptomycin.
122 For adipogenic differentiation, the cells were stimulated with DMEM/F12 glutaMax supplemented with

123 10% FBS, penicillin/streptomycin, 0.5 µg/mL insulin, 0.5 mM IBMX, 5 µM dexamethasone, 5 µM
124 rosiglitazone, 33 µM biotin (Sigma; B4639), and 17 µM pantothenic acid (Sigma; P5155) for 4 days.
125 The cells were then maintained in DMEM/F12 glutaMax supplemented with 10% FBS,
126 penicillin/streptomycin, 0.5 µg/mL insulin, 1 µM rosiglitazone, 33 µM biotin, and 17 µM pantothenic
127 acid. The medium was changed every other day. Fully differentiated cells (after 10 days) were used
128 for experiments.

129

130 **3. Results**

131 **3.1. TC-E treatment increases the expression of *Ucp1* mRNA in primary iWAT cells**

132 To evaluate the thermogenic activity of beige adipocytes, the stromal vascular fraction (SVF) isolated
133 from mouse inguinal WAT [iWAT; the largest subcutaneous (SQ) WAT] was differentiated into
134 adipocytes (primary iWAT cells) and then treated with isoproterenol (ISO; non-selective β-adrenergic
135 receptor agonist) or four kinds of PRMT1 inhibitors, namely, AMI-1 [15], MS023 [16], furamidine [17],
136 and TC-E [18]. As expected, *Ucp1* expression was robustly increased following ISO treatment but not
137 after AMI-1, MS023, or furamidine treatment (Figure 1A). However, unexpectedly, TC-E exposure
138 resulted in a strong upregulation of *Ucp1* expression to a level comparable with that observed
139 following ISO treatment (Figure 1A and 1B). Since the half maximal inhibitory concentration (IC50) of
140 TC-E is approximately 1.5 µM [18], we tested the effect of TC-E at a concentration of 1, 3 or 10 µM in
141 primary iWAT cells. TC-E greatly increased the expression of *Ucp1* at a dose of 10 µM and the effect
142 was absent at lower doses (1 or 3 µM) (Figure 1C). Moreover, 10 µM TC-E treatment led significant
143 increase in *Ucp1* mRNA and protein expressions up to 24 hours (Figure 1C and 1D). To examine the
144 depot-specific effect of TC-E, the SVFs isolated from iWAT, iBAT (classic brown adipocytes), and
145 eWAT (classic visceral white adipocytes) were treated with TC-E (Figure 1E). The effect of TC-E on
146 *Ucp1* mRNA expression in primary iWAT cells was abrogated in primary iBAT cells, whereas *Fgf21*
147 (encoding fibroblast growth factor 21) expression was induced by TC-E in both cell types. Gene
148 expression pattern of eWAT cells was similar to that of iWAT cells, although the increase by TC-E
149 treatment was marginal (Figure 1E). Given the increased *Ucp1* expression, we examined if TC-E
150 treatment increases thermogenesis of the cells using OLTAM [ODD-Luc (luciferase fused with the
151 oxygen-dependent degradation domain) based Thermogenic Activity Measurement] system that we
152 recently developed and reported to measure thermogenic activity of brown or beige adipocytes [14].
153 The result showed that TC-E treatment increased ODD-Luc activity to a level comparable with that
154 observed following ISO treatment, suggesting that TC-E enhances thermogenesis (Figure 1F).
155 However, mRNA levels of the genes related with mitochondria and the protein levels of OXPHOS
156 complexes were not altered by TC-E treatment (Figure 1G and 1H). These observations suggest that
157 TC-E strongly augments thermogenesis through increase of UCP1 expression (proton leak) without
158 changing mitochondrial content in primary iWAT cells.

159 **3.2. TC-E treatment activates the downstream molecules of PKA signaling**

This article is protected by copyright. All rights reserved

160 As PKA signaling is relevant to thermogenesis, we examined the dose- and time-dependent effects
161 of TC-E treatment on PKA activity in primary iWAT cells. Consistent with the effects on *Ucp1*
162 expression (Figure 1C), 10 μ M TC-E significantly increased PKA activity. This observation was
163 evident from Western blotting results using antibodies against phosphorylated PKA substrates as well
164 as phosphorylated p38, one of the substrates of PKA, in a time-dependent manner (Figure 2A and
165 2B). The TC-E-induced *Ucp1* and *Fgf21* expression in primary iWAT cells markedly reduced following
166 treatment with the selective PKA inhibitor, H-89, indicating that TC-E activates the thermogenic
167 pathway by inducing PKA activation (Figure 2C). We also examined whether TC-E treatment induces
168 lipolysis, as activated PKA not only upregulates the thermogenic pathway but also promotes lipolysis
169 through the activation of hormone-sensitive lipase (HSL) and Perilipin1 [9]. The PKA-dependent
170 phosphorylation of HSL at serine 563 and 660 increased following TC-E treatment, as observed with
171 ISO treatment (Figure 2D). In addition, the PKA-independent phosphorylation of HSL at serine 565,
172 which leads to HSL inactivation, was decreased [19]. Further, the PKA-dependent phosphorylation of
173 Perilipin1 at serine 522 was upregulated (Figure 2D and 2E), suggesting that TC-E treatment
174 increases lipolysis. Activation of lipolysis was further supported by the reduced size of lipid droplets
175 and increased release of glycerol, the split form of triacylglycerol, after ISO or TC-E treatment (Figure
176 2F and 2G).

177 **3.3. The effects of TC-E are independent of PRMT1 and beta-adrenergic receptors.**

178 The thermogenic effects of TC-E were not anticipated as the thermogenic activity in iWAT of
179 adipocyte-specific PRMT1 knockout (AP1KO) mice was clearly impaired after cold or β 3-adrenergic
180 receptor stimulation [10]. To clarify the discrepancy between the effects of TC-E and the phenotype of
181 AP1KO mice, primary iWAT cells from WT or AP1KO mice were incubated with TC-E (Figure 3A). As
182 a result, we found that the observed effects of TC-E (increased *Ucp1* and *Fgf21* expression, PKA
183 activity, and lipolysis) were unaltered by PRMT1 deficiency (Figure 3B-D). These results suggest that
184 effects of TC-E treatment were mediated in a PRMT1 independent manner.

185 Considering the canonical pathway of thermogenesis (β 3-adrenergic receptor–adenylyl cyclase–
186 cAMP–PKA), we speculated whether the TC-E-induced activation of PKA could be mediated by the
187 direct stimulation of β -adrenergic receptor. Therefore, we isolated primary iWAT cells from β -less
188 mice deficient for β 1, β 2, and β 3 adrenergic receptors [20] and incubated them with ISO, cAMP, or
189 TC-E. Given the lack of β receptors, no effects were observed following ISO treatment; however,
190 cAMP, a downstream molecule of β 3-adrenergic receptor, increased the expression of *Ucp1* and
191 *Fgf21*, as expected (Figure 3E). TC-E induced *Ucp1* and *Fgf21* expression even in β receptor-
192 deficient cells (Figure 3E), indicating that it does not directly stimulate β receptors. The significant
193 increase in the intracellular level of cAMP following ISO treatment was unaltered by TC-E treatment
194 (Figure 3F).

195 **3.4. TC-E potently works in human SQ cells**

196 We investigated the effects of TC-E on primary human adipocytes differentiated from SQ adipose

197 precursor cells. In human SQ cells, as seen in murine primary iWAT cells, TC-E treatment increased
198 *UCP1* and *FGF21* expression, PKA activity, and p38 and Perilipin1 phosphorylation (Figure 4A and
199 4B). We further examined the effects of TC-E on human SQ cells derived from two more different
200 individuals and found that TC-E increased the expression of thermogenic genes, although *UCP1*
201 induction was lower and not statistically significant in #3 (Figure 4C and 4D).

202

203 **4. Discussion**

204 In the present study, we demonstrate that treatment with TC-E, one of the chemical inhibitors of
205 PRMT1, results in the activation of the PKA-dependent thermogenic pathway in primary murine iWAT
206 cells and human SQ cells. SQ fat is the most widely distributed fat tissue, and individuals with a high
207 proportion of lower body SQ fats are metabolically healthy [21].

208 One of the important questions to understand human thermogenic adipocytes is if β 3-adrenergic
209 receptor is expressed in human SQ adipocytes [22-24]. Recent studies have shown that the β 3
210 agonist-mediated uptake of glucose, the typical fuel for thermogenesis, is absent in human SQ depots
211 [25,26]. However, thermogenic adipocytes seem to use not only glucose but also various other
212 molecules as fuel [27,28], and a significant portion of the energy expenditure occurs in the SQ fats
213 [29]. Furthermore, the expression of *UCP1* mRNA has been detected in human SQ depots [30],
214 suggesting that the activation of SQ fat may be potentially useful for the treatment of obesity.
215 However, the uncertainty related to the presence of β 3-adrenergic receptor on SQ adipocytes and the
216 possibility of inducing catecholamine resistance by repeated β 3 agonist treatment [31,32] have
217 highlighted the discovery of the drugs that work directly inside SQ adipocytes. Interestingly, the
218 activation of β 3-adrenergic receptor and TC-E treatment have convergences of mechanism; i) both
219 activate the expression of thermogenic genes, ii) both activate lipolysis, and iii) both mediate PKA
220 activation. Therefore, TC-E could be a potent activator of human SQ adipocytes. It is noteworthy that
221 TC-E treatment activated the downstream signaling molecules of β 3-adrenergic receptor even in
222 primary iWAT cells isolated from β -less mice.

223 As PRMT1 is required for the activation of thermogenic fat [10], we anticipated the downregulation of
224 the thermogenic program by PRMT1 inhibitors. However, TC-E treatment paradoxically increased
225 *Ucp1* and *Fgf21* mRNA expression in primary iWAT cells, whereas marginal effects were observed
226 with AMI-1, MS023, and furamide. In addition, the increase in *Ucp1* and *Fgf21* mRNA expression
227 following the treatment of wild-type iWAT cells with TC-E was comparable to that in PRMT1 knock-out
228 iWAT cells, indicating TC-E exerts thermogenic activity presumably not through PRMT1 inhibition. As
229 PKA activity increased from 15 min in primary iWAT cells following TC-E treatment, we measured the
230 intracellular levels of cAMP, which activates PKA. However, unlike ISO, TC-E treatment did not alter
231 cAMP level, indicating that TC-E activates PKA in a cAMP-independent manner. Studies have
232 revealed quite a few mechanisms related to cAMP-independent PKA activation [33-36]. Future
233 studies will, therefore, be needed to reveal the mechanism underlying the TC-E-mediated increase in

234 PKA activity.

235 TC-E, furamide, and AMI-1 are highly selective PRMT1 inhibitors, whereas MS023 is a type I
236 PRMTs inhibitor with affinity in the order of PRMT6 > PRMT8 > PRMT1 > PRMT4 > PRMT3. PRMT8
237 is exclusively expressed in the brain but not in the adipocytes [37]. PRMT4, also known as a
238 coactivator-associated arginine methyltransferase 1 (CARM1), and PRMT6 regulate adipogenesis by
239 interaction with peroxisome proliferator-activated receptor γ (PPAR γ) [38,39]. We observed that
240 MS023 treatment in our condition, failed to alter the expression of thermogenic genes probably
241 because PRMT4 and PRMT6 are not involved in the thermogenic program or owing to the composite
242 effects of MS023. Given the crucial role of type I PRMTs in various cellular processes, MS023
243 function is worth to be more investigated in the metabolisms of adipocytes.

244 In summary, TC-E treatment increases the expression of thermogenic genes most abundantly in
245 primary murine iWAT cells. TC-E also upregulates the PKA signaling pathway and lipolysis,
246 independently of PRMT1. The TC-E-induced expression of thermogenic genes and activation of
247 related signaling pathways are also observed in primary human SQ cells. Thus, TC-E may contribute
248 to the understanding of human SQ adipocyte thermogenesis and reveal the potential therapeutic
249 implication.

250

251 **Disclosure statement**

252 The authors declare no conflict of interest.

253

254 **Acknowledgments**

255 We thank Dr. Bradford Lowell for providing β -less mice and Dr. Seung-Hoi Koo for providing PRMT1^{fl/fl}
256 mice. This study was supported by a National Research Foundation of Korea (NRF) grant funded by
257 the Ministry of Science, ICT of Korea [grant number: NRF-2019R1C1C1007040 to D.-I. K.] and by the
258 Ministry of Education [grant number: NRF-2019R111A1A01060990 to M.-J. P.].

259 **References**

- 260 [1] van Marken Lichtenbelt, W.D., Vanhommerig, J.W., Smulders, N.M., Drossaerts, J.M.,
261 Kemerink, G.J., Bouvy, N.D., Schrauwen, P. and Teule, G.J. (2009). Cold-activated brown
262 adipose tissue in healthy men. *N Engl J Med* 360, 1500-8.
- 263 [2] Virtanen, K.A. et al. (2009). Functional brown adipose tissue in healthy adults. *N Engl J*
264 *Med* 360, 1518-25.

- 265 [3] Cypess, A.M. et al. (2009). Identification and importance of brown adipose tissue in adult
266 humans. *N Engl J Med* 360, 1509-17.
- 267 [4] Sharp, L.Z. et al. (2012). Human BAT possesses molecular signatures that resemble
268 beige/brite cells. *PLoS One* 7, e49452.
- 269 [5] Shinoda, K. et al. (2015). Genetic and functional characterization of clonally derived adult
270 human brown adipocytes. *Nat Med* 21, 389-94.
- 271 [6] Cypess, A.M. et al. (2013). Anatomical localization, gene expression profiling and functional
272 characterization of adult human neck brown fat. *Nat Med* 19, 635-9.
- 273 [7] Jespersen, N.Z. et al. (2013). A classical brown adipose tissue mRNA signature partly
274 overlaps with brite in the supraclavicular region of adult humans. *Cell Metab* 17, 798-805.
- 275 [8] Wu, J. et al. (2012). Beige adipocytes are a distinct type of thermogenic fat cell in mouse
276 and human. *Cell* 150, 366-76.
- 277 [9] Cannon, B. and Nedergaard, J. (2004). Brown adipose tissue: function and physiological
278 significance. *Physiol Rev* 84, 277-359.
- 279 [10] Qiao, X. et al. (2019). Protein Arginine Methyltransferase 1 Interacts With PGC1alpha and
280 Modulates Thermogenic Fat Activation. *Endocrinology* 160, 2773-2786.
- 281 [11] Hu, H., Qian, K., Ho, M.C. and Zheng, Y.G. (2016). Small Molecule Inhibitors of Protein
282 Arginine Methyltransferases. *Expert Opin Investig Drugs* 25, 335-58.
- 283 [12] Li, X., Wang, C., Jiang, H. and Luo, C. (2019). A patent review of arginine methyltransferase
284 inhibitors (2010-2018). *Expert Opin Ther Pat* 29, 97-114.
- 285 [13] Emont, M.P., Yu, H., Jun, H., Hong, X., Maganti, N., Stegemann, J.P. and Wu, J. (2015).
286 Using a 3D Culture System to Differentiate Visceral Adipocytes In Vitro. *Endocrinology* 156,
287 4761-8.
- 288 [14] Kim, D.I. et al. (2018). An OLTAM system for analysis of brown/beige fat thermogenic
289 activity. *Int J Obes (Lond)* 42, 939-945.
- 290 [15] Cheng, D., Yadav, N., King, R.W., Swanson, M.S., Weinstein, E.J. and Bedford, M.T. (2004).

- 291 Small molecule regulators of protein arginine methyltransferases. *J Biol Chem* 279, 23892-
292 9.
- 293 [16] Eram, M.S. et al. (2016). A Potent, Selective, and Cell-Active Inhibitor of Human Type I
294 Protein Arginine Methyltransferases. *ACS Chem Biol* 11, 772-781.
- 295 [17] Yan, L. et al. (2014). Diamidine compounds for selective inhibition of protein arginine
296 methyltransferase 1. *J Med Chem* 57, 2611-22.
- 297 [18] Bissinger, E.M. et al. (2011). Acyl derivatives of p-aminosulfonamides and dapsone as new
298 inhibitors of the arginine methyltransferase hPRMT1. *Bioorg Med Chem* 19, 3717-31.
- 299 [19] Anthonen, M.W., Ronnstrand, L., Wernstedt, C., Degerman, E. and Holm, C. (1998).
300 Identification of novel phosphorylation sites in hormone-sensitive lipase that are
301 phosphorylated in response to isoproterenol and govern activation properties in vitro. *J*
302 *Biol Chem* 273, 215-21.
- 303 [20] Bachman, E.S., Dhillon, H., Zhang, C.Y., Cinti, S., Bianco, A.C., Kobilka, B.K. and Lowell, B.B.
304 (2002). betaAR signaling required for diet-induced thermogenesis and obesity resistance.
305 *Science* 297, 843-5.
- 306 [21] Karpe, F. and Pinnick, K.E. (2015). Biology of upper-body and lower-body adipose tissue--
307 link to whole-body phenotypes. *Nat Rev Endocrinol* 11, 90-100.
- 308 [22] Vosselman, M.J., van der Lans, A.A., Brans, B., Wierdsma, R., van Baak, M.A., Schrauwen, P. and
309 van Marken Lichtenbelt, W.D. (2012). Systemic beta-adrenergic stimulation of
310 thermogenesis is not accompanied by brown adipose tissue activity in humans. *Diabetes*
311 61, 3106-13.
- 312 [23] Cypess, A.M. et al. (2015). Activation of human brown adipose tissue by a beta3-
313 adrenergic receptor agonist. *Cell Metab* 21, 33-8.
- 314 [24] Min, S.Y. et al. (2016). Human 'brite/beige' adipocytes develop from capillary networks,
315 and their implantation improves metabolic homeostasis in mice. *Nat Med* 22, 312-8.
- 316 [25] O'Mara, A.E. et al. (2020). Chronic mirabegron treatment increases human brown fat, HDL

- 317 cholesterol, and insulin sensitivity. *J Clin Invest* 130, 2209-2219.
- 318 [26] Jespersen, N.Z. et al. (2019). Heterogeneity in the perirenal region of humans suggests
319 presence of dormant brown adipose tissue that contains brown fat precursor cells. *Mol*
320 *Metab* 24, 30-43.
- 321 [27] Lynes, M.D. et al. (2017). The cold-induced lipokine 12,13-diHOME promotes fatty acid
322 transport into brown adipose tissue. *Nat Med* 23, 631-637.
- 323 [28] Simcox, J. et al. (2017). Global Analysis of Plasma Lipids Identifies Liver-Derived
324 Acylcarnitines as a Fuel Source for Brown Fat Thermogenesis. *Cell Metab* 26, 509-522.e6.
- 325 [29] Muzik, O., Mangner, T.J., Leonard, W.R., Kumar, A., Janisse, J. and Granneman, J.G. (2013).
326 15O PET measurement of blood flow and oxygen consumption in cold-activated human
327 brown fat. *J Nucl Med* 54, 523-31.
- 328 [30] Lim, J., Park, H.S., Kim, J., Jang, Y.J., Kim, J.H., Lee, Y. and Heo, Y. (2020). Depot-specific
329 UCP1 expression in human white adipose tissue and its association with obesity-related
330 markers. *Int J Obes (Lond)* 44, 697-706
- 331 [31] Arner, P. (1999). Catecholamine-induced lipolysis in obesity. *Int J Obes Relat Metab Disord*
332 23 Suppl 1, 10-3.
- 333 [32] Mowers, J., Uhm, M., Reilly, S.M., Simon, J., Leto, D., Chiang, S.H., Chang, L. and Saltiel, A.R.
334 (2013). Inflammation produces catecholamine resistance in obesity via activation of PDE3B
335 by the protein kinases IKKepsilon and TBK1. *Elife* 2, e01119.
- 336 [33] Lu, A. and Hirsch, J.P. (2005). Cyclic AMP-independent regulation of protein kinase A
337 substrate phosphorylation by Kelch repeat proteins. *Eukaryot Cell* 4, 1794-800.
- 338 [34] Ma, Y., Pitson, S., Hercus, T., Murphy, J., Lopez, A. and Woodcock, J. (2005). Sphingosine
339 activates protein kinase A type II by a novel cAMP-independent mechanism. *J Biol Chem*
340 280, 26011-7.
- 341 [35] Kohr, M.J., Traynham, C.J., Roof, S.R., Davis, J.P. and Ziolo, M.T. (2010). cAMP-independent
342 activation of protein kinase A by the peroxynitrite generator SIN-1 elicits positive inotropic

343 effects in cardiomyocytes. *J Mol Cell Cardiol* 48, 645-8.

344 [36] Melville, Z. et al. (2017). The Activation of Protein Kinase A by the Calcium-Binding Protein
345 S100A1 Is Independent of Cyclic AMP. *Biochemistry* 56, 2328-2337.

346 [37] Taneda, T., Miyata, S., Kousaka, A., Inoue, K., Koyama, Y., Mori, Y. and Tohyama, M. (2007).
347 Specific regional distribution of protein arginine methyltransferase 8 (PRMT8) in the
348 mouse brain. *Brain Res* 1155, 1-9.

349 [38] Yadav, N., Cheng, D., Richard, S., Morel, M., Iyer, V.R., Aldaz, C.M. and Bedford, M.T. (2008).
350 CARM1 promotes adipocyte differentiation by coactivating PPARgamma. *EMBO Rep* 9,
351 193-8.

352 [39] Hwang, J.W., So, Y.S., Bae, G.U., Kim, S.N. and Kim, Y.K. (2019). Protein arginine
353 methyltransferase 6 suppresses adipogenic differentiation by repressing peroxisome
354 proliferator-activated receptor gamma activity. *Int J Mol Med* 43, 2462-2470.

355
356
357

358 **Figure legends**

359 **Figure 1. TC-E increases *Ucp1* and *Fgf21* mRNA expression in primary iWAT cells.**

360 (A) Primary iWAT cells were incubated with ISO (10 μ M), AMI-1 (10 μ M), MS023 (10 μ M), furamidine
361 (100 μ M), or TC-E (10 μ M) for 4 h, and the expression of *Ucp1* mRNA was measured ($n=3$). (B)
362 Molecular structure of TC-E. (C, D) Cells were incubated with TC-E for 4 h or indicated time intervals.
363 (C) The expression of *Ucp1* mRNA was measured ($n=3$). (D) UCP1 protein expression was analyzed.
364 β -Actin was used as the loading control. (E) The TC-E-induced expression of *Ucp1* and *Fgf21*
365 mRNAs was determined in primary iWAT, iBAT, and eWAT cells (4 h treatment). (F) Adenoviral-
366 OLTAM-transduced primary iWAT cells were incubated with 10 μ M ISO for 5 h or 10 μ M TC-E for 24
367 h and then luciferase activity was measured ($n=4$). (G) Primary iWAT cells were incubated with 10 μ M
368 TC-E for 4 h, and the mRNA expression of genes related with mitochondria were measured ($n=3$). (H)
369 Primary iWAT cells were incubated with 10 μ M TC-E for indicated time intervals. Protein expressions
370 of OXPHOS complex were analyzed. β -Actin was used as the loading control. All values are
371 presented as mean \pm SEM. * $p < 0.05$, ** $p < 0.01$, and *** $p < 0.001$. *n.s.* (not significant).

372 **Figure 2. TC-E activates the PKA signaling and lipolysis pathway in primary iWAT cells.**

This article is protected by copyright. All rights reserved

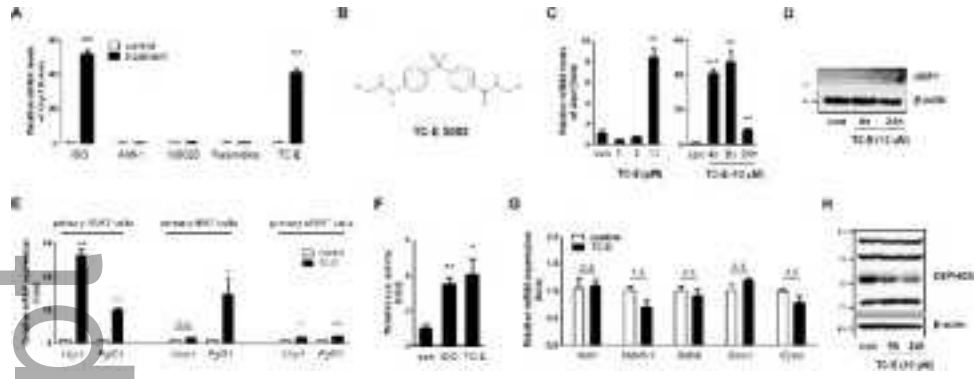
373 (A, B) Primary iWAT cells were incubated with TC-E (A) at different doses for 4 h or (B) 10 μ M
374 concentration of TC-E for different time intervals. Protein levels were analyzed. β -Actin was used as
375 the loading control. (C) Cells were pre-incubated with H-89 (50 μ M) or vehicle for 1 h and treated with
376 TC-E or vehicle for 4 h. mRNA levels were measured ($n=4$). $*p < 0.05$ and $***p < 0.001$, control versus
377 TC-E; $\#p < 0.05$ and $###p < 0.001$, TC-E versus TC-E + H-89. (D) Protein levels in primary iWAT cells
378 incubated with TC-E, ISO (10 μ M), or vehicle were analyzed. (E,F) Immunofluorescence analysis of
379 primary iWAT cells incubated with ISO (10 μ M for 1 h), TC-E (10 μ M for 4 h), or vehicle. Signals for
380 phospho-Perilipin1 are shown in red and counterstaining of lipid droplets using BODIPY is shown as
381 green (scale bar = 20 μ m). (E) Content of phospho-Perilipin1 and (F) size of lipid droplets were
382 quantified. (G) Glycerol levels in the medium of primary iWAT cells incubated with ISO (10 μ M for 1
383 h), TC-E (10 μ M for 1 h), or vehicle were measured ($n=3$). $*p < 0.05$ and $**p < 0.01$ versus control.

384 **Figure 3. Thermogenic properties of TC-E in primary iWAT cells are independent of PRMT1 and**
385 **β -adrenergic receptor.**

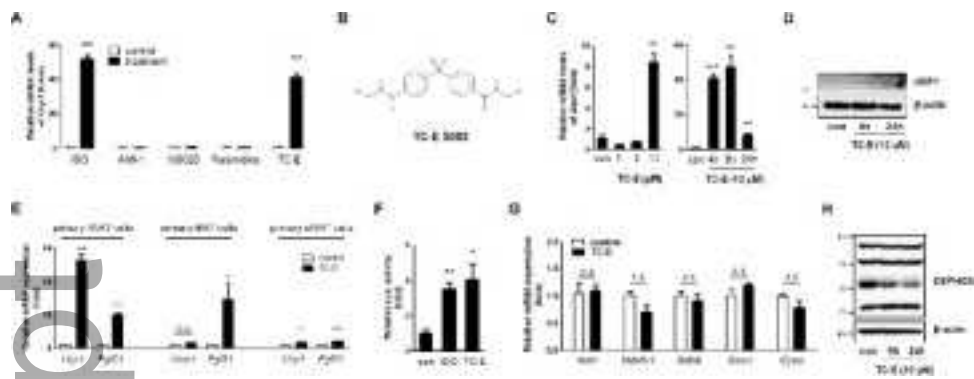
386 (A, B) The mRNA levels were measured in primary iWAT cells of wild-type (WT) or adipocyte-specific
387 PRMT1 knockout (AP1KO) mice ($n=3$). (B) Primary iWAT cells treated with 10 μ M TC-E or vehicle for
388 4 h were analyzed ($n=3$). (C) Protein levels in primary iWAT cells incubated with 10 μ M TC-E were
389 analyzed. HSP90 was used as the loading control. (D) Glycerol levels in the medium of primary iWAT
390 cells incubated with TC-E (10 μ M for 4 h) were measured ($n=3$). (E) Primary iWAT cells were isolated
391 from β -less mice and incubated with ISO (10 μ M), cAMP (500 μ M), or TC-E (10 μ M) for 4 h. The
392 mRNA levels were measured ($n=3$). (F) Primary iWAT cells were incubated with ISO (10 μ M), TC-E
393 (10 μ M), or vehicle for 10 min. Intracellular cAMP levels were analyzed ($n=3$). $*p < 0.05$ and $***p <$
394 0.001 . *n.s.* (not significant).

395 **Figure 4. TC-E increases thermogenic pathway in human SQ cells.**

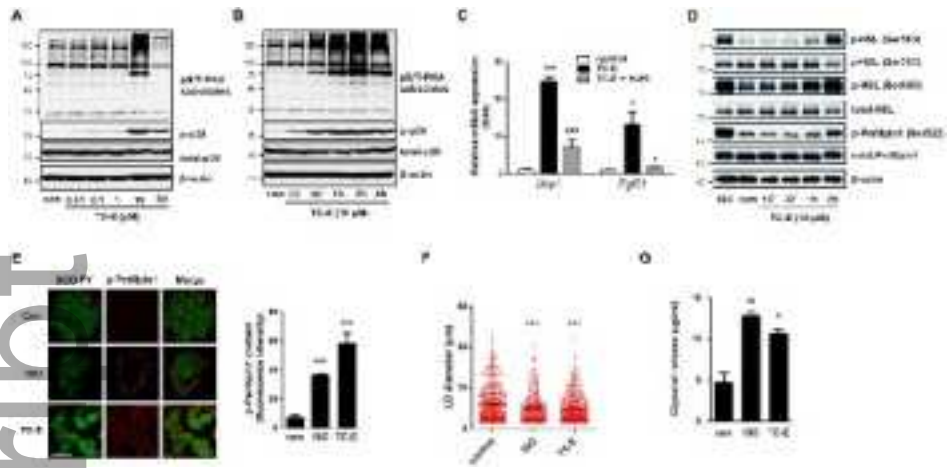
396 (A, B) Human subcutaneous (SQ) cells (#1) were analyzed. (A) Human SQ cells were incubated with
397 10 μ M TC-E or vehicle for 4 h and the mRNA levels were measured ($n=3$). (B) Human SQ cells were
398 incubated with 10 μ M TC-E for indicated time intervals. Protein levels were measured. β -Actin was
399 used as the loading control. (C, D) mRNA levels were measured in human SQ cells (#2 or #3) ($n=3$).
400 $*p < 0.05$, $**p < 0.01$, and $***p < 0.001$. *n.s.* (not significant).



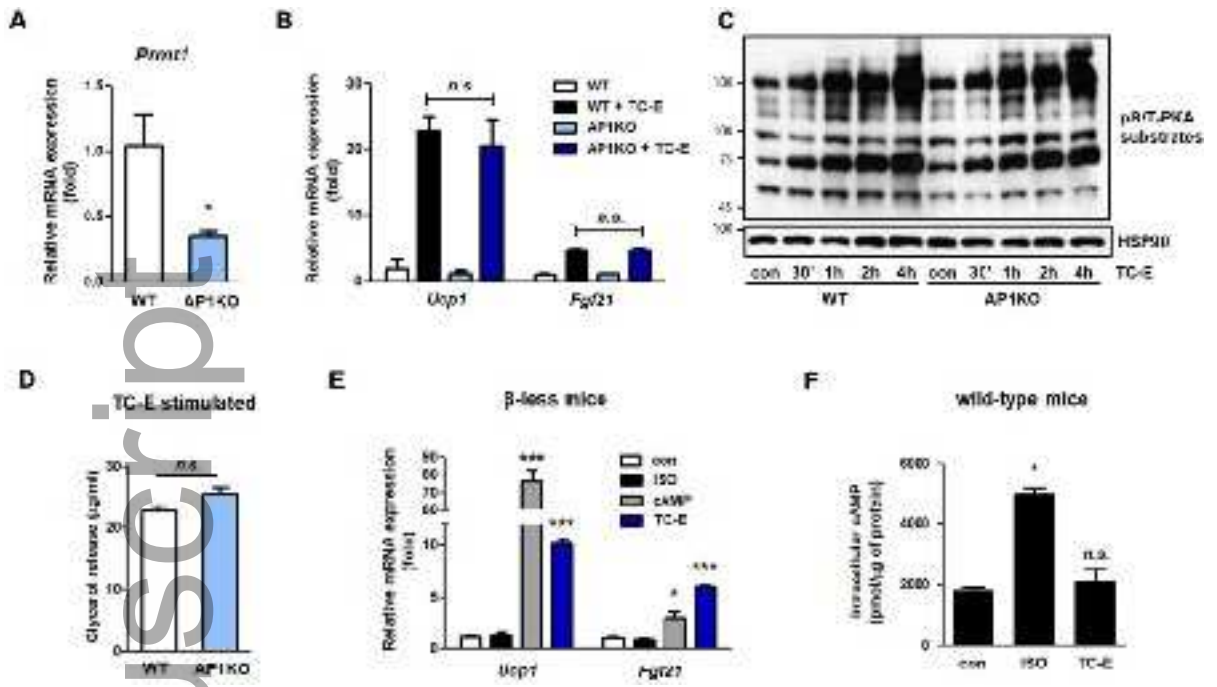
feb2_13900_f1.tif



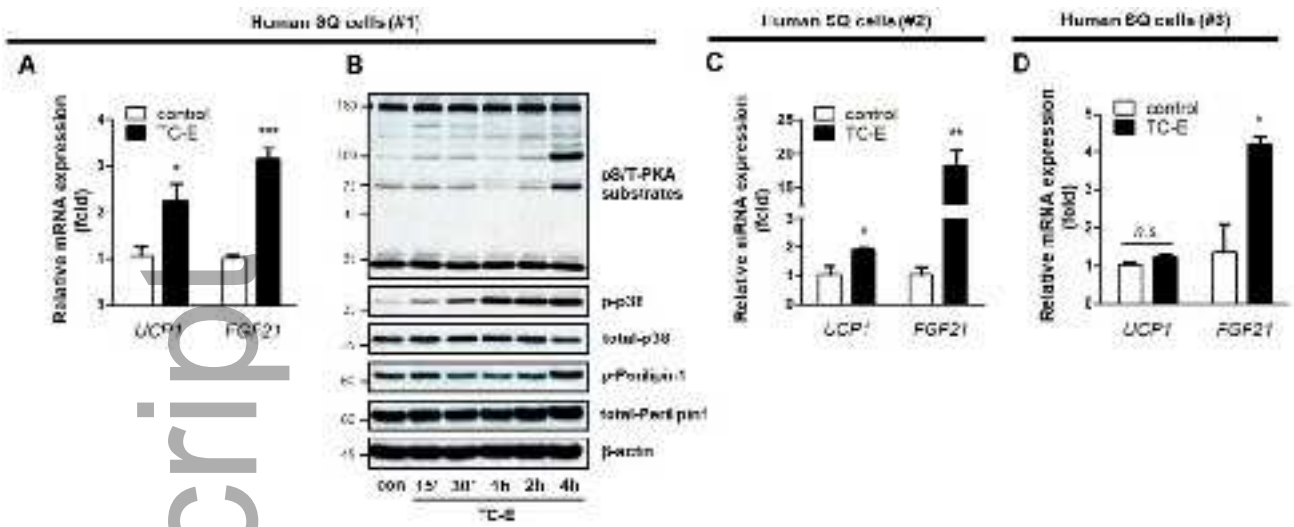
feb2_13900_f1.tif



feb2_13900_f2.jpg



feb2_13900_f3.jpg



feb2_13900_f4.jpg